# A probabilistic detailed level approach to flood risk assessment in the Scheldt estuary

J. Blanckaert
*IMDC, Antwerp, Belgium*

L. Audoorn
*Department of Applied Mathematics, University of Ghent, Belgium*

ABSTRACT: It is commonly understood that computational limitations imply the adoption of considerable simplifications in flood risk analysis. Those simplifications focus either on the hydrodynamic model, e.g. through substitution by a response surface, or on the boundary conditions, e.g. by ignoring some variables or drawing a limited number of design storms with a set probability. Drawbacks of this approach include an unreliable quantification of uncertainties and a questionable extrapolation to extremely low probabilities. This paper covers an investigation towards the achievability of a Monte Carlo approach for flood risk assessment by means of a hydrodynamic model. Efforts were made to stick to the well-known physical laws and interrelationships. This contribution fits in the framework of a societal cost-benefit analysis of flood protection measures in the Scheldt basin. It can be concluded that, if computing power is substantially available, the quasi Monte Carlo method is a reliable and comprehensible tool for flood risk assessment.

## 1 INTRODUCTION

During 3/1/1976 900 houses were inundated by a storm tide in Flanders, Belgium. This disaster gave rise to the conception of the smaller Flemish equivalent of the at that time almost finished Dutch Delta plan : the so-called Sigma plan for the tidal reach of the Scheldt and its tidal tributaries. Due to a decreasing public awareness of inundation risk and an economic crisis this Sigma plan has never been completed. The planned storm surge barrier was never constructed and of the other measures, river embankment elevations and implementation of a number of controlled inundation areas, 80 % have been carried out nowadays (2004). In 2001 the Flemish Parliament decided to develop a long term vision upon the development of the Scheldt estuary, integrating security against flooding, nature development and accessibility of the port of Antwerp. The resolution stated that the Sigma plan had to be updated by means of a risk approach resulting in a societal cost-benefit analysis. In this cost-benefit analysis different alternative protection schemes are compared to the reference scheme, which is the completed original Sigma Plan (except for the storm surge barrier).

As explained by Bulckaen et al. (2005), the cost is computed by considering the investment for the flood protection works as well as operational and maintenance expenditure. On the benefit side, the avoided flood losses in the river basin, as well as nature development, are estimated. This paper focusses on the probabilistic part of the cost-benefit calculation, i.e. the assessment of avoided inundation damage. To fully assess the flood risk, which can be represented by an expected mean annual damage value, a flood damage probability distribution is necessary. This distribution should be computed by simulation of all possible storm conditions by means of a hydrodynamic model of the entire river basin, followed by the calculation of losses due to every single storm condition. Since the hydrodynamic branched 1D model of the Scheldt and its tributaries, inluding all possible floodplains, is quite an extensive numerical calculation tool, its computing speed is limited. Hence, simulation of all possible storm conditions, like the Monte Carlo method whose simplicity is in big contrast with its computing time, is rarely used in hydrodynamics. For this reason simplified methods are often adopted, either by substituting the detailed hydrodynamic model with a fastly computing response model, e.g. a response surface or a neural network, or by simplification of the stochastic model of the storm conditions, e.g. by ignoring variables that may appear insignificant, by ignoring uncertainties or by considering only a limited number of design storms.

Each simplification involves a number of drawbacks. A hydrodynamic model is based on physical laws, i.e. continuity and momentum equations, friction loss laws and erosion formulae for breaching. It is most unlikely that a response surface or neural

network can display the same results as a detailed hydrodynamic model for all potential boundary conditions, particularly when regarding extreme conditions. Moreover one can expect that in different floodplains, completely different substituting models are bound to be built. On the other hand, using a detailed hydrodynamic model and simplifying the stochastic behaviour of the boundary conditions involves similar disadvantages. A rather big number of variables play an important role in flood generation, e.g. storm surge, astronomic tiding, wind direction and wind speed producing an additional wind setup, time shifts, rainfall run-off,... It is impossible to figure out which of them is predominant, as their share in the resulting water level is random. Furthermore, designing composite storms with set return periods that retain this return period after simulation is not a simple task.

Simplifications require an extensive reliability analysis of the effects of the assumptions, which is a time consuming task and of which the result remains uncertain. In this study a methodology is investigated which discards the simplified approach and copes with possible computational problems. This paper covers the achievability of a Monte Carlo approach for flood risk assessment by means of a hydrodynamic model.

## 2 METHODOLOGY

A hierarchical Monte Carlo scheme is used to generate samples with sets of boundary conditions and estimate the resulting probability distribution of the occurring damage. A sufficiently large amount of samples will be required to get an accurate estimate of the probability distribution function of the damage and related mean annual risk.

The hydrodynamic model is bound by an upstream and a downstream boundary condition. The latter is made of two parts : a time series of water levels and a time series of wind speeds and wind directions. The water level itself is the superposition of several constituents of stochastic nature : the astronomic tiding Ah(t) (astronomic high water level AHW, astronomic low water level, and astronomic tide profile), storm surge coming from the North Sea and a time shift $\Delta t_{AHW\text{-}S}$ between the maximum storm surge $S^{max}$ and AHW. The storm surge is again composed of two stochastic variables : the maximum storm surge $S^{max}$ and a typical (standardized) time profile $S_0(t)$. To account for non-linear depth effects the storm surge is filtered of these effects, leading up to a new variable, denoted by subscript 0, e.g. $S_0^{max}$. The wind storm consists of three components : the wind direction r, the maximum wind speed $w^{max}$ and a standardized time profile w(t). The downstream boundary condition is completed by a random time shift $\Delta t_{S\text{-}w}$ between $S_0^{max}$ and $w^{max}$.

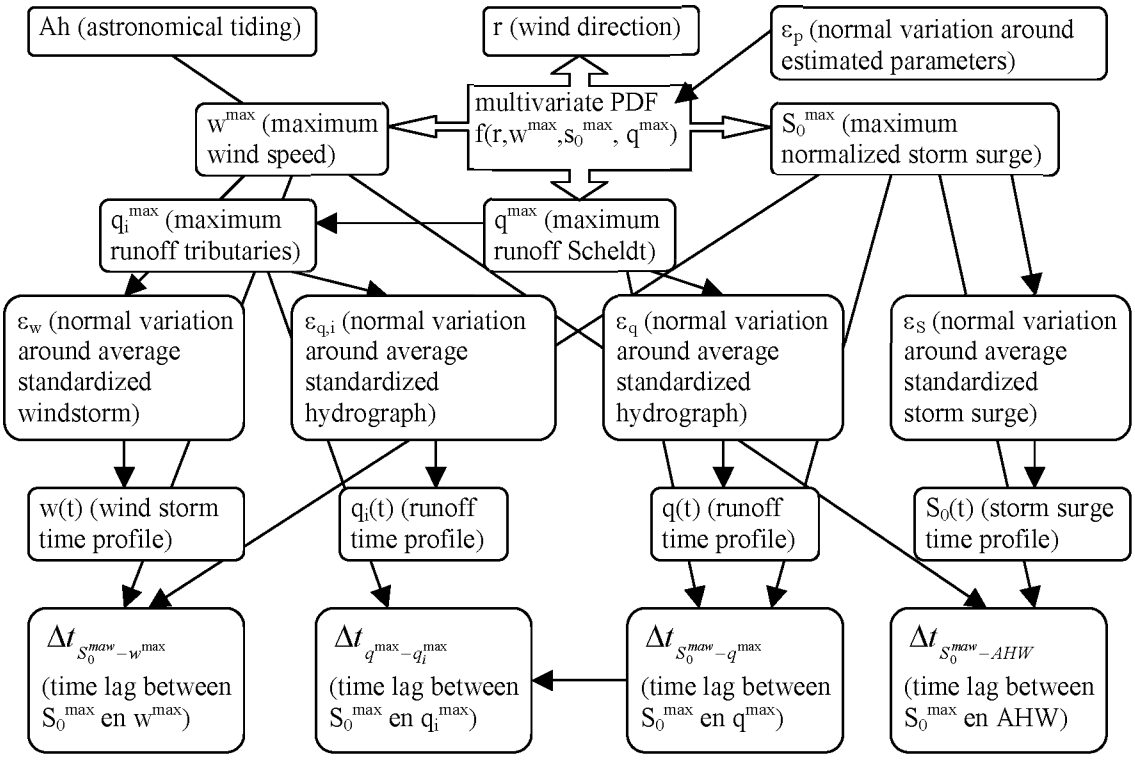


Figure 1. Schematic representation of main and secondary variables and their mutual dependencies

The upstream boundary conditions of the hydrodynamic model consists in one time series of run-off discharges q(t) at the upper limit of the main branch of the Scheldt and five time series $q_i(t)$ (i = 1 to 5) at the influent tributaries. Each time series is composed of three constituents : a maximum discharge $q^{max}$ or $q_i^{max}$, a standardized hydrograph q(t) or $q_i(t)$, and time shifts $\Delta t_{S-q}$ between $S_0^{max}$ and $q^{max}$ and $\Delta t_{q-qi}$ between $q^{max}$ and $q_i^{max}$.

A complete overview of all 24 variables is displayed in Figure 1, indicating the mutual dependencies by arrows. Section 4 covers an extensive description of the different random variables and the statistical inferences. For all probability distributions the parameter uncertainty has been calculated, denoted in Figure 1 by $\varepsilon_p$.

The hierarchical Monte Carlo method executes a sampling in serial order: first random number sequences are applied to sample parameter values out of the calculated variation about the estimated parameters, next new random numbers are used to calculate actual values for the different variables by means of their probability distribution with the formerly sampled parameter values. This routine is repeated for all variables, first for the independent (Ah(t)) or multivariately modeled variables (r, $w^{max}$, $S_0^{max}$, $q^{max}$), and subsequently for the dependent variables.

As a result, the boundary condition time series of the hydrodynamic model are obtained, each set of which having a specific probability of occurrence. Hydrodynamic simulation of the storm samples results in flood depths in the floodplains of the hydrodynamic model, for which damages can be computed through a GIS analysis (see section 3). With the selected number of samples, an empirical cumulative probability distribution of flood damage is estimated.

We round this section off with a word about the random numbers. The random numbers must be, at least to a good approximation, realizations of independent and uniformly distributed random variables. In this study quasi random sequences are applied for the sampling routines. Quasi random number sequences show less discrepancy than (pseudo)random numbers, which implies greater uniformity. When sampling extreme values by means of a threshold model it is clear that quasi random numbers efficiently cover the Peak Over Threshold variable's domain, including extremely high values (Coles, 2001, Krykova, 2003).

## 3 HYDRODYNAMIC MODEL

A general overview of the Scheldt basin is shown in Figure 2. A hydrodynamic branched 1D model was set up of the Scheldt and its tributaries (Bulckaen, 2005), starting at the river mouth (Vlissingen, NL) and covering the entire tidal reach of the river up to the upstream limit near Melle, and including the downstream part of the main tributaries (Dender, Demer, Dijle, Zenne and Nete). The estuary is modeled with multiple interconnected branches in a quasi 2D approach. All possible inundation areas are enclosed (through Digital Area Maps), seperated from the main river by dikes which can be overtopped and in which breach development is modeled by means of a breach erosion algorithm.

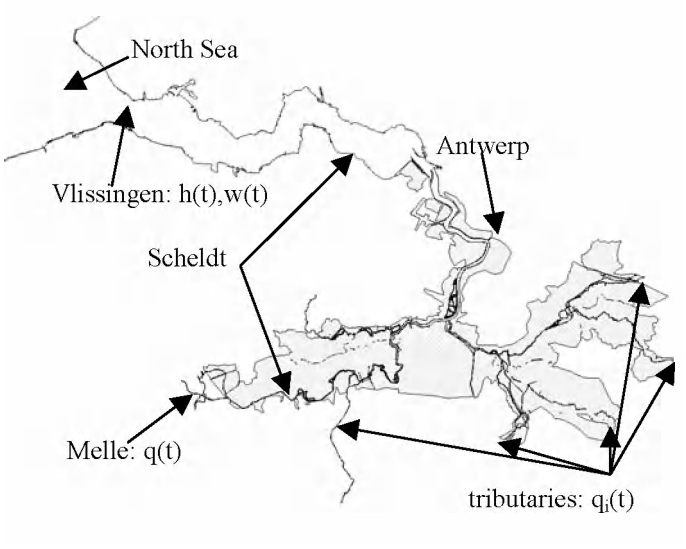


Figure 2. General overview of the tidal Scheldt with its potential flood areas and the location of the model boundary conditions.

No additional uncertainty about the calculated water levels h(t) is accounted for in the analysis. This uncertainty can be considered more than an order of magnitude smaller than the uncertainties to the other involved variables.

For reasons of automation, related to the large number of samples to be simulated, use is made of total damage functions which correspond to damage cells. All possible inundation areas are broken down in different smaller damage cells, each of which belonging to a single output node of the hydrodynamic model. An example is displayed in Figure 3. The total damage function in fact is an average over the cell around a specific node. In doing so, the time consuming step of GIS applications is avoided. The outcome of a total damage function is the damage in Euro (Vanneuville & Maeghe, 2004), directly related to the maximum water depth in the node of the hydrodynamic model in the flooded area. A database is built up in which total damage functions are stored for 628 flood cells defined in the hydrodynamic model, which results in a density of about 10 flood cells for each kilometer of the river. A few examples are given in Figure 4. These damage functions reflect the impact of a dense populated city center, an industrial area, a residential area and an agricultural area at different locations along the Scheldt basin.

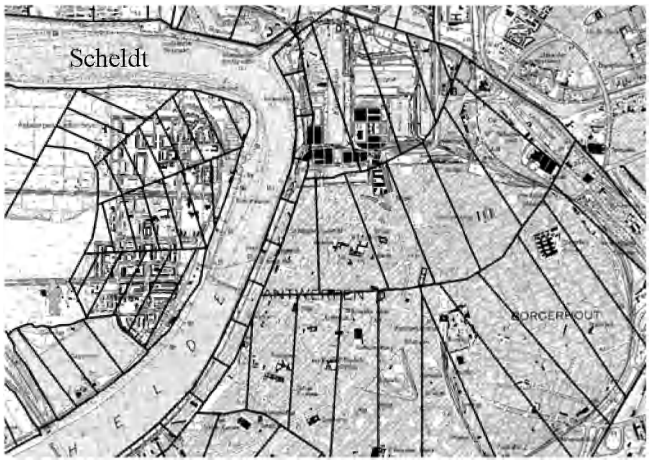


Figure 3. Flood and damage cells in city centre of Antwerp.

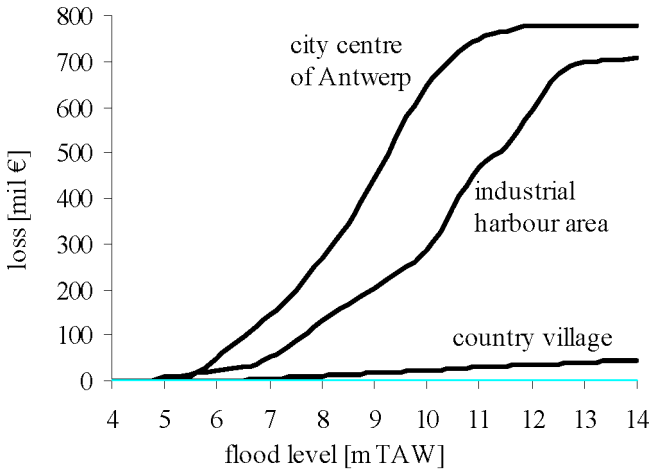


Figure 4. Loss functions for three different types of land use

## 4 BOUNDARY CONDITIONS

### 4.1 *Astronomic water level Ah*

Tidal movement at the downstream end of the model, Vlissingen, is composed of 95 harmonic components, the largest period of which being 18.6 years. This lunar nodal tide component has yet a considerable tide amplitude of 8 cm in Vlissingen. A hindcast of 18.6 years of predicted tide levels – carried out by RIKZ – on a 10' time step yields in 13,177 mutually differing tide cycles, which is an accurate representative for the population of all possible tide cycles. Hence, it was unnecessary to fit some kind of a probability distribution to any variable describing the astronomic tide profile (high water level HW, low water level LW,…), and any variations in rising and falling limbs have been accounted for. A simple uniform sampling out of the 13,177 tide cycles is sufficient.

### 4.2 *Storm surge S*

For this study a time series of 14 years (1987-2000) of recorded water level data in Vlissingen was available with a sample frequency of 10 minutes. Storm surges were computed by subtracting the predicted astronomic tide levels from the corresponding gauged water levels.

Next, the hypothesis was adopted that lunar and solar positions with respect to the Earth are independent to the meteorological conditions. As a consequence every sampled astronomic tide cycle – out of the population of 13,177 possible tide cycles – could coincide with any possible storm surge height. Due to non-linear tide-surge interactions and shallow water effects this is not the case in the recorded surge data set, as shown in Figure 5. The dashed bars in Figure 5 represent the mean storm surge as a function of the predicted water level classes. This mean is calculated by considering all storm surge values exceeding 40 cm, which is considered as a reliable significance threshold for storm surge calculations by Trouw (2002), for which the corresponding predicted water level is found in the same 20 cm interval. The dashed line in Figure 5 is a simple linear regression over the dashed columns. The dependency of maximum storm surge to the predicted water level is obvious. This appears to be in contradiction with the earlier assumption of independency of astronomical and meteorological conditions. Therefore an attempt was made to filter depth related effects (Silvester, 1974) out of the storm surge time series. This was done by dividing every storm surge record by the actual gauged water level en multiplying it by the mean water level in Vlissingen. The result is shown in Figure 5 by means of the grey coloured bars and regression line. The latter makes the assumption of independency more likely.

Still from Figure 5 a cyclic water level dependent behaviour is suggested, presumably created by non-linear tide-surge effects. Those effects are partly accounted for by introducing the stochastic time lag $\Delta t_{AHW\text{-}S}$ between the peak value $S_0^{max}$ of the storm surge and the nearest astronomical high water AHW, covered in section 4.5.

Random storm surges are generated through a multivariate extreme value distribution (see section 4.6) which pictures the joint occurrence of a peak storm surge, a peak run-off discharge and a peak wind speed coming from a certain wind direction. As explained in section 4.6 the multivariate distribution is computed in two steps: first a marginal distribution is fit to the univariate set of Peak Over Threshold (POT) values and after that the mutual dependencies are assessed out of a set of simultaneous POT values of the different dependent variables.

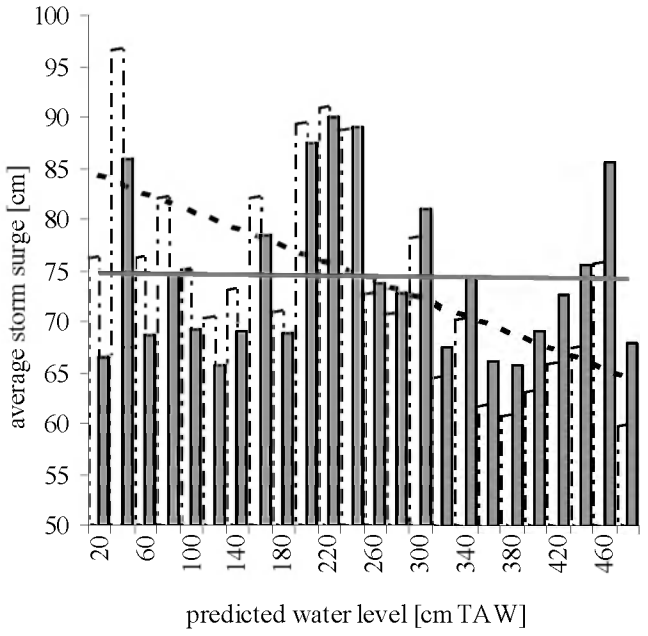


Figure 5. Water level dependent storm surges. Mean observed surges S in dashed bars, linear regression over entire predicted water level range in dashed line. Homogenized surges $S_0$ in coloured bars, linear regression in grey line. The latter shows independence of predicted water level for $S_0$.

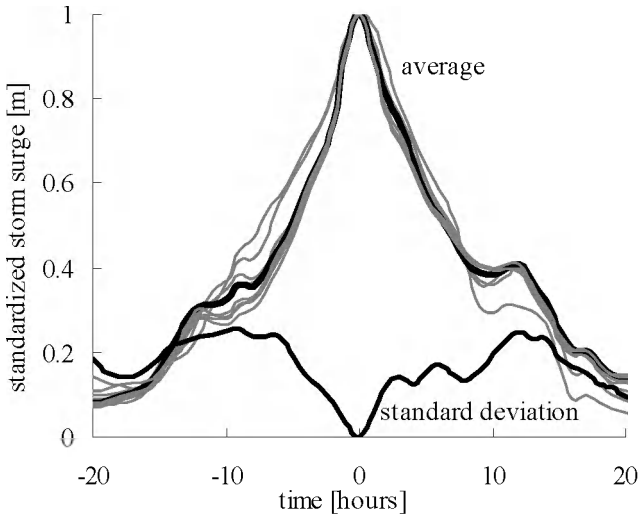


Figure 6. Standardized storm surge profiles with average and standard deviation in bold face.

The combination of storm surge with high wind velocities is important in the Scheldt estuary, since the wind – if blowing from western directions – can generate a considerable additional wind setup. Moreover, major storm surges in the southern North Sea never occur with wind speeds coming from land. Hence, the wind direction is of major importance, and southern and eastern wind directions could be excluded from the analysis, since no threshold excesses could be found in the recorded surge and wind dataset. Subsequently 8 directions were left : N, NNW, NW, WNW, W, WSW, SW and SSW. The storm surge POT-values are subdivided over those wind directions according to the corresponding wind speed (see section 4.3).

POT values for storm surge are selected by applying the thresholds listed in Table 1 and combining 2 independency criteria : a maximum inter-event level and an minimum inter-event time span. By examining storm surge registrations over 40 years, Sas (1984) concluded that two consecutive storm events can be considered as independent if the time span between both events is more than 60 hours and the storm surge has fallen to zero. Applying these criteria, 252 independent events could be selected in the 14 years filtered storm surge time series, the 30 biggest of which being used to design a standardized storm surge profile. By scaling down the calculated storm surge time profiles between 0 en 1, a mean standardized storm surge profile could be derived as well as a standard deviation, as shown in Figure 6.

As part of the storm events generation, surge time series will be created by random sampling a peak surge $S_0^{max}$ value through its statistical distribution, next random sampling of a standardized surge profile out of the normal distributed variation in Figure 6, and finally the multiplication of the standardized surge profile with te sampled $S_0^{max}$ leads up to an actual surge sample.

### 4.3 *Wind speed and wind direction*

Hourly wind speed and wind direction data is made available by the KNMI, over a time span of 40 years. Wind speed and storm surge display a considerable correlation, which will be discussed in section 4.6.

Preliminary to all calculations, wind directions have been transformed by calculating a wind speed weighted moving average over 6 hours to avoid rapid and random fluctuations. Computation of statistical inferences is less complicated if the wind direction is treated as a discrete variable, attaching all major wind speeds to 8 possible directions : N, NNW, NW, WNW, W, WSW, SW and SSW.

Two series of POT values were selected in consideration of the computation of the joint probability distribution in section 4.6: one based on joint occurrence of high wind speeds and high storm surges, and the other for assessing the marginal extreme value distribution for wind speed.

The latter has been built by selecting POT-values – threshold levels are listed in Table 1 – out of the complete 40 years record using an inter-event criterium of 48 hours to ensure the independency between the selected extremes. This minimum time span was proposed by Palutikov (Palutikov et al.,

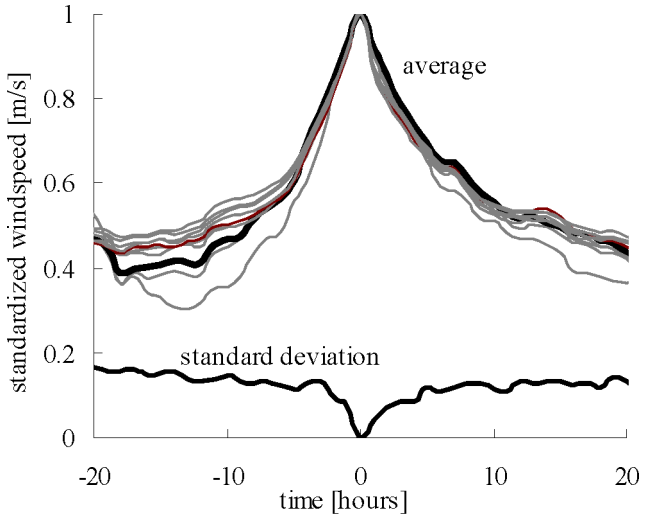


Figure 7. Standardized wind speed profiles with average and standard deviation in bold face.

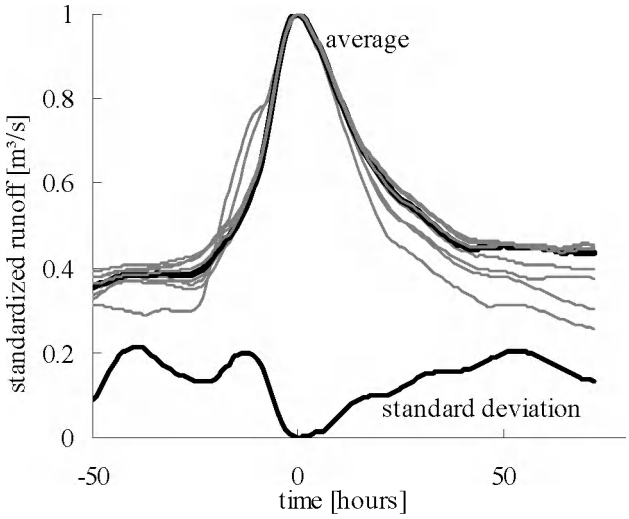


Figure 8. Standardized run-off hydrograph with average and standard deviation in bold face.

1999). Accordingly wind directions were taken out of the moving average wind direction series.

The joint probability tracking POT value series was composed by selecting the highest wind speeds $w^{max}$ and the according wind direction in a 48 time span to both sides of every storm surge POT value. Therefore the maximum wind speed $w^{max}$ in a 60-hour time span before each of the 252 storm surge POT values $S_0^{max}$ is kept, together with the corresponding wind direction r and the time shift $\Delta t_{S-w}$ between the peak storm surge and the maximum run-off discharge. Statistical inference for $w^{max}$ is covered in section 4.6. The random variation in $\Delta t_{S-w}$ could be explained by $S_0^{max}$ through a linear regression line with a normal distributed prediction interval.

The wind storms, corresponding to the 30 most severe $w^{max}$ values, have been standardized to a mean unit windstorm and a normal variation about the mean was adopted by computing the standard deviation produced by the 30 selected wind storms. The result is illustrated by Figure 7, where some of the individual standardized hydrographs are drawn in grey. The mean unit wind storm and the standard deviation about this mean are shown in bold face.

As part of the storm events generation, wind storms will be created by random sampling of $w^{max}$ through its statistical distribution, next random sampling of a standardized wind storm out of the normal distributed unit wind storm variation and multiplication of both. Another random sampling of a time shift $\Delta t_{S-w}$ determines the downstream boundary for the regarded storm event.

### 4.4 *Run-off discharges*

The upstream end of the tidal reach of the Scheldt is bounded by a couple of sluices. If the maximum sluice flow capacity is exceeded, the excess run-off discharges will be holded in the upstream river basin, possibly subject for flooding outside the study area. Anyhow, the discharge input into the model is bounded by the sluices' capacity and exploratory model simulations revealed that this maximum discharge was unable to cause any bank overtopping along the tidal reach of the Scheldt, if happening without a significant storm surge. This has been verified by historical flood reports and local press releases. Hence, only run-off discharges accompanied by a significant storm surge have been involved in the analysis, thus allowing to restrict the multivariate extreme value model to a bivariate GPD, with different parameters for each discrete wind direction, covered in section 4.6. By selecting the highest run-off discharges in a reasonable time span around every storm surge POT value, additional effects of run-off volumes on flood depths during storm tides are satisfactory accounted for. Therefore, the maximum run-off discharge $q^{max}$ in a 60-hour time span before and after each of the 252 storm surge POT values $S_0^{max}$ are kept, together with the time shift $\Delta t_{S-q}$ between the peak storm surge and the maximum run-off discharge. Statistical inference for $q^{max}$ is covered in section 4.6. Again, the random variation in $\Delta t_{S-q}$ could be explained by $S_0^{max}$ through a linear regression line with a normal distributed prediction interval.

The hydrographs, corresponding to the 30 most severe $q^{max}$ values, have been standardized to a mean unit hydrograph and a normal variation about the mean was adopted by computing the standard devia-

tion produced by the different selected hydrograph. The result is illustrated in Figure 8, where some of the individual standardized hydrographs are drawn in greyscale. The mean unit hydrograph and the standard deviation about this mean are shown in bold face.

As part of the storm events generation, hydrographs will be created by random sampling of $q^{max}$ through its statistical distribution, next random sampling of a standardized hydrograph out of the normal distributed unit hydrograph variation and the multiplication of the standardized hydrograph with te sampled $q^{max}$ leads up to an actual hydrograph sample. Another random sampling of a time shift $\Delta t_{S\text{-}q}$ determines the upstream boundary for the regarded storm event.

### 4.5 *Brief overview of other variables*

The remaining random variables to reckon with are: the time lag $\Delta t_{AHW\text{-}S}$ of the astronomic high water AHW with respect to the peak storm surge $S_0^{max}$, the peak run-off discharges $q_i^{max}$ from the tributaries, the corresponding standardized hydrograph time profiles $q_i(t)$ and time lags $\Delta t_{qi\text{-}q}$ between the tributary peak discharge and the upper Scheldt peak discharge.

The analysis of the time shifts $\Delta t_{AHW\text{-}S}$ is based on the selection of 252 measured events. Since it was impossible to explain $\Delta t_{AHW\text{-}S}$ by a regression model, likely due to nonlinear tide-surge effects (see section 4.2), an empirical density function was adopted to model the random time shift $\Delta t_{AHW\text{-}S}$.

The 5 main tributaries – Dender, Demer, Dijle, Zenne and Nete – are indicated in Figure 2. For each tributary the maximum run-off discharge $q_i^{max}$ was modeled by a linear regression with predictor $q^{max}$, the maximum discharge in the upstream Scheldt catchment (see section 4.4), with normal distributed prediction bounds. The reasonably high correlation between the tributary flows and the upper Scheldt run-off can be attributed to their common origin, the rainfall/run-off events, which are generally moving eastwards. Time shifts $\Delta t_{qi\text{-}q}$ appeared to be independently normally distributed. For each tributary a standardized run-off hydrograph was computed the way it has been for the upper Scheldt catchment in section 4.4.

### 4.6 *Statistical inferences*

A multivariate model has been set up to represent the joint occurrence of extremes of the 4 main variables : peak storm surge $S_0^{max}$, peak run-off hydrograph $q^{max}$, peak wind speed $w^{max}$ and wind direction r.

As discussed in section 4.4, it is possible to account for the effect of upstream run-off by drawing a conditional distribution to the 252 independent vectors of componentwise extremes ($r, w^{max}, S_0^{max}, q^{max}$). Since the wind direction has been treated as a discrete variable, dividing the wind rose in 22.5°-sections, a conditional formulation was appropriate either. Eventually the derivation of multivariate distribution upon 4 variables could be confined to a bivariate threshold excess model for every considered wind direction r:

$$\begin{aligned}&\Pr\left\{r, w^{max}, S_0^{max}, q^{max}\right\} = \\ &\Pr\{r\}\cdot\Pr\left\{w^{max}, S_0^{max}\middle| r\right\}\cdot\Pr\left\{q^{max}\middle| w^{max}, S_0^{max}, r\right\}\end{aligned} \quad (1)$$

where the second factor denotes the bivariate extreme value distribution, for which the Generalized Pareto Distribution has been chosen.

As a preliminary step, the shape parameter $\xi$, the scale parameter $\sigma$ and the threshold u have been estimated for the marginal GPD distributions of $S_0^{max}$ and $w^{max}$,

$$H(X-u_r) = \begin{cases} 1-\left(1+\dfrac{\xi_r(X-u_r)}{\sigma_r}\right)^{-\frac{1}{\xi_r}} & if\ \xi \neq 0 \\ 1-\exp\left(-\dfrac{X-u_r}{\sigma_r}\right) & if\ \xi = 0 \end{cases}, \quad (2)$$

after grouping the corresponding POT values to the considered wind directions. A summary of the estimated parameters is given in Table 1. All estimations where carried out by maximising the parametric log-likelihood function (Kotz & Nadarajah, 2000).

Table 1. Parameter estimates for marginal GPD distributions.

| wind direction | $S_0^{max}$ | | | $w^{max}$ | | |
|---|---|---|---|---|---|---|
| | $\xi_r$ | $\sigma_r$ [cm] | $u_r$ [cm] | $\xi_r$ | $\sigma_r$ [m/s] | $u_r$ [m/s] |
| N | 0 | 19.8 | 40 | 0 | 1.58 | 9 |
| NNW | 0 | 37.2 | 55 | 0 | 2.16 | 8 |
| NW | 0 | 41.1 | 45 | 0 | 1.7 | 10 |
| WNW | 0 | 23.5 | 90 | -0.33 | 3.53 | 12 |
| W | 0 | 24.6 | 105 | -0.3 | 3.76 | 13 |
| WSW | 0 | 18.8 | 102 | -0.14 | 2.42 | 15 |
| SW | -0.54 | 47.2 | 50 | 0 | 2.24 | 14 |
| SSW | 0 | 19.8 | 40 | 0 | 1.86 | 14 |

In the next step the dependency between both storm surge and wind speed has to be determined. This was done through the symmetric logistic dependence structure, with copula

$$C(u,v) = \exp\left[-\left\{(-\log u)^{1/\alpha_r} + (-\log v)^{1/\alpha_r}\right\}^{\alpha_r}\right]. \quad (3)$$

where u en v denote a uniform transformation of the marginal distribution functions (Coles et al. 1999, Kotz & Nadarajah, 2000) :

$$(u,v) = \left\{F_{S_0^{max}}(s), F_{w^{max}}(w)\right\}, \quad 0 \le u, v \le 1 \quad (4)$$

where $F_X$ denotes the marginal GPD of variable X.

The parameter $\alpha$ determines the strength of dependence between storm surge and wind speed in any particular wind direction : $\alpha = 1$ gives independence; decreasing $\alpha$ leads to increased dependence with perfect dependence arising in the limit as $\alpha = 0$. Table 2 shows the estimated dependency levels for different wind directions, carried out by means of a log-likelihood maximisation.

Table 2. Estimates of copula parameter.

| wind direction | $\alpha_r$ |
|---|---|
| N | 0.88 |
| NNW | 0.66 |
| NW | 0.89 |
| WNW | 0.61 |
| W | 0.70 |
| WSW | 0.95 |
| SW | 0.97 |
| SSW | 0.86 |

Ultimately we can write the second factor in Equation (1), the joint distribution function for every wind direction:

$$\Pr\left\{w^{\max}, S_0^{\max} \middle| r\right\} = C_r\{u, v\} \tag{5}$$

where r denotes the use of the appropriate parameter values for the different wind directions, listed in Table 1 and Table 2.

The parameter estimates for the run-off GPD didn't show significant mutual differences throughout the considered wind directions, nor any dependency to storm surge or wind speed. Therefore a simple marginal (unconditional) GPD was fit to the 252 maximum hydrograph discharges corresponding to the POT storm surges. Doing so possible dependencies are pragmatically accounted for, since only peak discharges are considered if both the corresponding storm surge and wind speed exceed their thresholds. As explained in section 4.4, inundation by only high run-off discharges is not to be expected due to limited upstream sluice capacity. Consequently, the third factor in Equation (1) has been approximated by :

$$\begin{aligned}&\Pr\left\{q^{\max} \middle| w^{\max}, S_0^{\max}, r\right\} \approx \\ &\Pr\left\{q^{\max} \middle| w^{\max} > u_{r,w}, S_0^{\max} > u_{r,s}\right\}\end{aligned} \tag{6}$$

where $u_{r,w}$ and $u_{r,s}$ denote the thresholds for wind speed and storm surge, respectively, listed in Table 1. Maximum likelihood parameter estimation of Equation (2) resulted in $\xi = 0$, $\sigma = 79$ m³/s and $u = 1$ m³/s for the run-off GPD.

Wind directions were modelled by their empirical probabilities according to the 252 selected events. The first factor in Equation (1) becomes

$$\Pr\{r\} = \frac{i_r}{252} \tag{7}$$

where $i_r$ denotes the number of 252 events with wind direction r.

For all estimated parameters confidence intervals were calculated by means of the profile log-likelihood method (Coles 2001). Prior to the random sampling of any variable, a random sampling of a parameter value has been carried out, according to the principles of the hierarchical Mont Carlo method.

### 4.7 *Storm sample generation*

Samples of the random variables are taken by means of the quasi random number sequences. Therefore a N by k quasi random number matrix has been built, where N denotes the number of samples to be calculated and k the total number of variables, including the parameter estimation uncertainties.

Every single synthetic storm sample is composed by evaluating the inverted CDF of each variable at the value of the random number in the corresponding location of the quasi random number matrix. The first random number, listed in the first column of the matrix, is used to select the wind direction of the current storm sample. After setting the wind direction, all bivariate GPD parameter estimations in Table 1 en Table 2 are known. For each parameter $\alpha$, $\xi$ and $\sigma$ a confidence interval has been calculated, out of which the next 3 random numbers sample the applicable parameter values. The subsequent random number is used to draw a random peak storm surge and peak wind speed out of the bivariate GPD with the earlier set parameter values. The same procedure is repeated for all other main and secondary variables, i.e. the run-off discharges, the time profiles and the time shifts.

Finally, the synthetic storm sample events are made up by combining all sampled variables. An example is drawn in Figure 9. The sampled astronomic tide Ah(t) is repeated several times, taking into account the sampled time shift $\Delta t_{AHW\text{-}S}$ between astronomic high water level and the maximum filtered storm surge. After applying the inverse filter-procedure to account for the depth related effects the storm surge S(t) is added to Ah(t) to have a water level time series h(t). Similar routines are carried out for the other variables. As schematically shown in Figure 2, each synthetic event contains a downstream boundary water level time series h(t), several upstream boundary flow time series q(t) and a downstream wind storm time series w(t) with a specified wind direction r.

The storm sample generation algorithm can be verified by a comparison of the maximum storm sample water levels with gauged storm tide high water levels at the downstream boundary of the hydrodynamic model. A stationary 40 years time series of high water levels is available in Vlissingen (Blanckaert, 2003), out of which POT values have

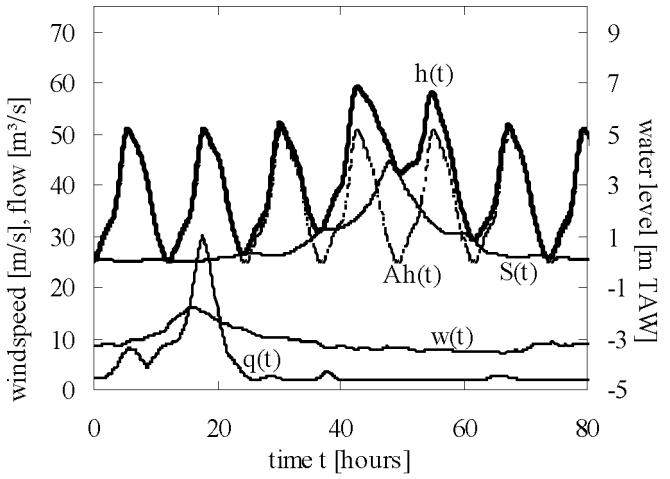


Figure 9. Time series of storm sample variables.

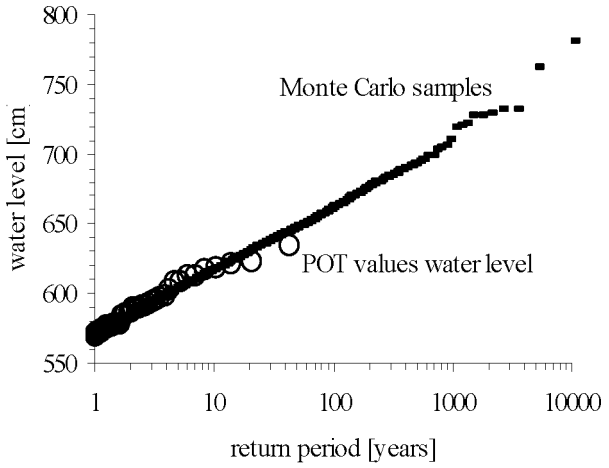


Figure 10. Probability plot of generated storm samples and POT values of gauged water levels in Vlissingen.

been selected through the independency criterium of a minimum inter-event timespan of 60 hours. In a probability plot, the peak water levels of the N Monte Carlo samples should coincide with the selected POT-values. Apparantly this is the case, as shown in Figure 10.

## 5 FLOOD LOSS ASSESSMENT

In Belgium there are no legal impositions related to the necessary degree of protection against flooding. The typical topography in the Scheldt basin implies that there is no asymptotical upper limit for the risk value as with ever increasing flood events always more (big) cities will be inundated, causing discontinuous leaps in the loss distribution as well as the risk value. Therefore the project team decided to calculate flood damages up to a return period of 10,000 years, what is felt the maximum level of protection flood defence systems should offer (Bulckaen et al., 2005).

With 252 events crossing the multivariate thresholds in a time span of 14 years, or an average of 18 events a year, at least 180,000 storm samples are necessary to achieve results for a return period of 10,000 years.

Prior to the Monte Carlo flood simulations an extensive sensitivity analysis has been carried out with the hydrodynamic model, to establish a number of joint criteria to all boundary conditions, defining a secure no-inundation-causing field in the multivariate boundary condition domain. This could be rapidly done with a fast model without any flood cells, since only water levels in the main river reach determine whether inundation is arising or not. Applying these criteria to the 180,000 random generated storm samples, 13,182 events were selected that might give rise to inundation somewhere in the tidal Scheldt basin.

Simulation of those 13,182 events was required to draw the damage probability distribution. Hydrodynamic simulation and damage calculation throughout the entire basin has been fully automatically done by a battery of 5 workstations in a 15 days batch process. Simulation crashes were automatically fixed by rerunning and decreasing the calculation time step.

The whole process was repeated for two alternative schemes for the updated Sigma Plan : first the reference scheme (the complete original Sigma Plan except for the storm surge barrier), which is expected to be the actual situation in 2010, and second the same configuration with additional controlled inundation areas, reduced tide areas and dike elevations (Couderé et al., 2005).

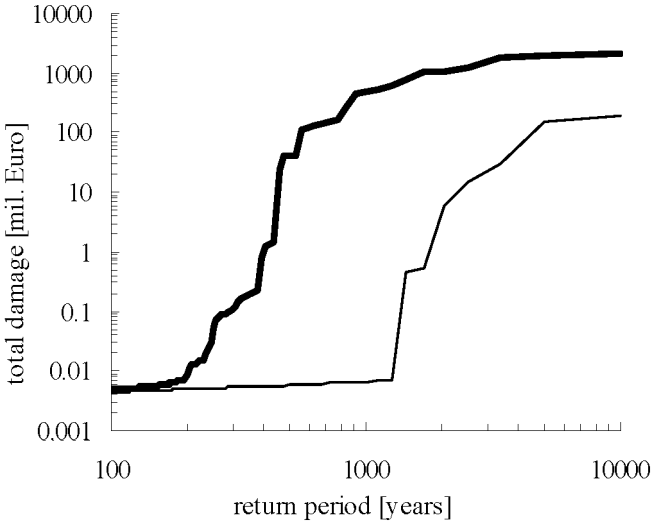


Figure 11. Empirical CDF of total damage to be expected in the Flemish part of the tidal Scheldt catchment, for two different scenario's. In bold : current situation, in fine print: taking flood protecting measures (controlled inundation areas, dike elevation).

## 6 RESULTS

Of the 13,182 simulated events, 1100 actually caused any flood damage in the reference scheme, and only half of this number in the modified option. The resulting empirical damage probability distributions are drawn in Figure 11. The risk value can be assessed by computing the area under the distribution curves. From Figure 11 it is obvious that damage probabilities are much smaller in the modified option, for reason that it contains additional flood protecting measures.

The results are being used to evaluate the costs and benefits of different alternatives, taking into account changing meteorological circumstances (Bulckaen, 2005). Therefore additional calculations are currently executed to compute the damage probability distributions for the year 2100.

## 7 CONCLUSIONS

In this study the achievability of a Monte Carlo simulation through a 1D hydrodynamic model, dealing with 24 random variables and statistical uncertainties, is investigated. If computing power is substantially available, the quasi Monte Carlo method is a reliable and comprehensible tool for flood risk assessment. When evaluating many different flood protection schemes, modeled with as much hydrodynamic models, this approach can be very time consuming, compared to a simplified method with a limited number of design or composite storms. Nevertheless, since the stochastic model of design storms is radically simplified and uncertainties are only pragmatically accounted for, the Monte Carlo method can be a useful tool to estimate the accuracy of the design storm method. In the societal cost-benefit analysis of the Sigma plan, a big number of possible flood protection measures are being considered. Therefore, composite storms are being composed in order to permit rapid risk assessment. For two protection schemes, i.e. the reference scheme and the modified scheme (see section 5), the Monte Carlo results will be used to interpret the composite storm approach.

In spite of the vast number of executed statistical calculations, probability assessment could be improved. The applied parametric method for likelihood estimation of the bivariate GPD could be replaced by the semiparametric estimation provided by Dixon & Tawn (1995). Furthermore it is recommended to consider the huge uncertainties involved in quantifying the total damage functions, which is neglected in the present study due to a lack of information.

## 8 ACKNOWLEDGEMENTS

This study was funded by the Flemish Administration of Waterways and Marine Affairs, as part of a large-scale societal cost-benefit analysis of flood defence measures in the Flemish part of the tidal Scheldt basin.

Numerous data sets were made available by the Dutch National Institute for Coastaland Marine Management (RIKZ), the Royal Dutch Meteorological Institute (KNMI) and Flanders Hydraulics Research. K. Doekes (RIKZ) is gratefully acknowledged for making available the hindcast time series of astronomic water levels at Vlissingen.

The ingenuity of the hydrodynamic modeling team at IMDC, the useful comments of K. Maeghe (Flanders Hydraulics Research) are highly appreciated.

Many statistical calculations, particularly the maximum likelihood fits and the quasi random numbers generation, have been carried out using the R language and environment for statistical computing (R Foundation for statistical Computing, Vienna, Austria). Hydrodynamic simulations were executed with Mike 11 software (DHI Water & Environment, Hørsholm, Denmark).

## 9 REFERENCES

Beirlant, J., Teugels, J.L. & Vynckier, P. 1996. Practical analysis of extreme values. Leuven: Leuven University Press.

Blanckaert J., 2003. Actualisatie van het Sigmaplan: deelopdracht 3, volume 1a: Statistiek Scheldebekken. Antwerp : Flemish Administration of Waterways and Marine Affairs (in Dutch).

Bulckaen, D., Smets, S., De Nocker, L., Broekx, S., Dauwe, W. 2005. Updating of the Belgian Sigma plan on a risk-assessment basis. Third International Symposium on Flood Defence (in prep.).

Couderé, K., Gommers, A. & Dauwe, W. 2005. Strategic environmental assessment for the Sigma plan. Third International Symposium on Flood Defence (in prep.).

Coles, S. 2001. An introduction to statistical modeling of extreme values. London: Springer-Verlag.

Coles, S., Heffernan, J. & Tawn, J. 1999. Dependence measures for multivariate extremes. *Extremes 2*: 339-365.

Dixon, M.J. & Tawn, J.A. 1995. A semiparametric model for multivariate extreme values. *Statist. Comput 5*, 215-225.

Huthnance, J.M. Predicting storm surges and other sea level changes. CCMS Proudman Oceanographic Laboratory.

Kotz, S. & Nadarajah, S. 2000. Extreme value distributions, theory and applications. London: Imperial College Press.

Krykova, I. 2003. Evaluating of path-dependent securities with low discrepancy methods. Worcester: Polytechnic Institute.

Palutikov, J.P., Brabson, B.B., Lister, D.H. & Adcock, S.T. 1999. A review of methods to calculate extreme wind speeds. *Meteorological Applications*, 6, 119-132.

Roskam, A.P., Hoekema, J. & Seijffert, J.J.W. 2000. Richtingsafhankelijke extreme waarden voor HW-standen, golfhoogten en golfperioden. Den Haag: Dutch National Institute for Coastal and Marine Management (RIKZ) (in Dutch).

Sas, M. 1984. Frequency of occurrence of storm surges in an estuary : a stochastic approach. 19th International Conference on Coastal Engineering. Houston : ASCE.

Silvester, R. 1974. Coastal Engineering 2. Amsterdam: Elsevier.

Trouw, K., Blanckaert, J., Verwaest, T., Hurdle, D., Van Alboom, W., Monbaliu, J., De Rouck, J., De Wolf, P., Willems, M., Sas, M., Decroo, D. & van Banning, G. 2004. Extreme hydrodynamic boundary conditions near Ostend. 29th ICCE-conference (in press).

Vanneuville, W. & Maeghe, K. 2002. Risicobenadering bij waterbeheersingsplannen, methodologie en case study Denderbekken. Antwerp: Flemish Administration of Waterways and Marine Affairs, Flanders Hydraulics Research (in Dutch).